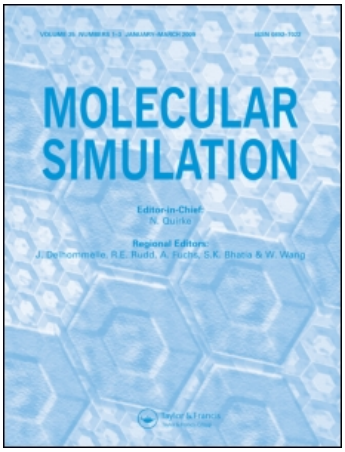

Molecular Simulation
Publication details, including instructions for authors and subscription information:
http://www.informaworld.com/smpp/title~content=t713644482

Charge effects on alkanes and the potential applications in selective catalysis: insights from theoretical studies

Gang Yang[a]; Chengbu Liu[b]; Xiuwen Han[a]; Xinhe Bao[a]
[a] State Key Laboratory of Catalysis, Dalian Institute of Chemical Physics, Chinese Academy of Sciences, Dalian, P.R. China [b] Institute of Theoretical Chemistry, Shandong University, Jinan, P.R. China

First published on: 13 August 2009

To cite this Article Yang, Gang , Liu, Chengbu , Han, Xiuwen and Bao, Xinhe(2010) 'Charge effects on alkanes and the potential applications in selective catalysis: insights from theoretical studies', Molecular Simulation, 36: 3, 204 — 211, First published on: 13 August 2009 (iFirst)
To link to this Article: DOI: 10.1080/08927020903177666
URL: http://dx.doi.org/10.1080/08927020903177666

Molecular Simulation
Vol. 36, No. 3, March 2010, 204–211

Taylor & Francis
Taylor & Francis Group

Charge effects on alkanes and the potential applications in selective catalysis: insights from theoretical studies

Gang Yang[a]*, Chengbu Liu[b], Xiuwen Han[a] and Xinhe Bao[a]

[a]*State Key Laboratory of Catalysis, Dalian Institute of Chemical Physics, Chinese Academy of Sciences, 457 Zhongshan Road, Dalian 116023, P.R. China;* [b]*Institute of Theoretical Chemistry, Shandong University, Jinan 250100, P.R. China*

(*Received 3 April 2009; final version received 2 July 2009*)

Methane structures endowed with different charges have been experimentally observed, but understanding of them currently remains rather limited. With the aid of *ab initio* calculations, a systematic work was carried out on the methane structures with different charges (0, ±1, ±2) as well as on the structures of the neutral methane molecule bound to anions (O^{2-} and F^-) and cations (Na^+ and Mg^{2+}). The geometry of the neutral methane species was found to be well reserved in the negatively charged structures but severely distorted in the positively charged ones. The binding modes of the neutral methane species with cations (Na^+ and Mg^{2+}) and anions (O^{2-} and F^-) are threefold and onefold, respectively. The smallest and largest elongations of the C—H bonds in methane were observed in the binding with Na^+ and O^{2-}, respectively. According to the C—H bond dissociation energies (BDE1s), the dissociation pathways were determined for all the structures, and are in agreement with the experimental data. It was further revealed that the first C—H BDE1s are heavily dependent on the charges of the methane species. Through the charge effects, the activations of the first C—H bonds in methane become facile; in addition, the selective activations and conversions can be fine-tuned as well. Accordingly, the charge effects have the potential to be employed in the effective utilisation of alkanes.

Keywords: *ab initio* calculations; alkanes; charge effects; C—H bonds; selective activations

1. Introduction

A series of pioneering researches has been carried out on dipole-bound anions [1–5]. The glycine zwitterion in the gas phase cannot exist independently and will be converted into neutral isomers in a barrierless way. With the attachment of an excess electron, Simons and his collaborators [4] found that the glycine zwitterion became a local minimum on the potential energy surface. The subsequent work of Ai et al. [6] indicated that the ionisations can stabilise the glycine zwitterion as well. Unlike the structures previously reported [1–6], the cations and anions of methane are greatly destabilised by charge effects, i.e. the attachments or ionisations of electrons. This is caused by the strong Jahn–Teller effects [7,8] since the highest occupied molecular orbitals (HOMOs) of methane are threefold degenerate. Through consistent efforts, the cations of the singly and doubly photoionised methane were observed experimentally [9–13]. Very recently, the electrons have also been successfully attached to the neutral methane structure [14]. To date, no systematic investigations have been performed on neutral and charged methane structures. In this work, neutral and charged methane structures were optimised with *ab initio* calculations. Molecular orbital analyses were used to aid our understanding of the intrinsic instabilities of the charged methane structures. The C—H dissociation energies of these structures were determined by considering all the possible dissociation pathways. In addition, the first and second ionisation energies (IEs) and electron affinities (EAs) of methane were calculated and compared with the data available to us as well as the corresponding values of the noble gas Ne. To further understand the charge effects on C—H bond dissociations, the structures of methane bound to the various anions (e.g. O^{2-} and F^-) and cations (e.g. Na^+ and Mg^{2+}) were also investigated. Owing to the noticeable influences of the first and second C—H bond dissociations, the charge effects can be used to selectively activate the alkanes, including methane. As is known to us, the effective utilisation of alkanes still represents one of the current challenges in catalysis [15–18].

2. Computational details

All the *ab initio* calculations were performed with the Gaussian03 software package [19]. Three types of structures were involved in this work. (A) The neutral and charged methane structures, which are designated as $^{M}CH_4(n)$. *M* in superscript and *n* in parentheses represent spin multiplicity and charge, respectively. (B) The dissociated fragments of the $^{M}CH_4(n)$ structures as well as the structures used for comparisons, e.g. noble gas Ne,

*Corresponding author. Email: dicpyanggang@yahoo.com.cn

ISSN 0892-7022 print/ISSN 1029-0435 online

DOI: 10.1080/08927020903177666
http://www.informaworld.com

methanol (CH_3OH) as well as their related structures. (C) The structures of the neutral $^1CH_4(0)$ bound to anions and cations as well as the related dissociated products. All these structures were optimised at the MP2/6-311++G(d,p) level, and the harmonic vibrational frequencies were employed at the same level to check whether these structures are energy minima or not. The structures of the former two types (A) and (B) were further refined under the CCSD(T)/6-311++G(d,p) level of theory.

The natural bond orbital program [20] embodied in the Gaussian 03 software package was used to obtain the Wiberg bond indices (bond orders), which are a measure of bond strengths [21].

The C—H bond dissociation energies (BDE1s) of the various $^MCH_4(n)$ structures were calculated:

$$\mathrm{BDE1} = E[^{M1}\mathrm{CH_3}(n1)] + E[^{M2}\mathrm{H}(n2)] - E[^{M}\mathrm{CH_4}(n)], \quad (1)$$

where $M1$, $n1$ and $M2$, $n2$ denote the spin multiplicities and charges of the dissociated products CH_3 and H, respectively.

3. Results and discussion

3.1 Structural analysis of $^MCH_4(n)$

The charges (n) and spin multiplicities (M) of the $^MCH_4(n)$ structures are presently considered to fall within the ranges of [−2, +2] and [1,3], respectively. Eight possible combinations resulted, corresponding to $^1CH_4(0)$, $^3CH_4(0)$, $^2CH_4(-1)$, $^1CH_4(-2)$, $^3CH_4(-2)$, $^2CH_4(1)$, $^1CH_4(2)$ and $^3CH_4(2)$. All these structures were optimised with MP2/6-311++G(d,p) and CCSD(T)/6-311++G(d,p) methods, and the geometries at the two theoretical levels were found to be in excellent agreement. The frequencies calculated at the MP2/6-311++G(d,p) level indicated that $^1CH_4(0)$, $^2CH_4(-1)$, $^1CH_4(-2)$, $^2CH_4(1)$ and $^3CH_4(2)$ are energy minima whereas $^3CH_4(0)$, $^3CH_4(-2)$ and $^1CH_4(2)$ are not. The results were supported by the previous results: the neutral methane structure is known to exist without unpaired electrons corresponding to $^1CH_4(0)$. The double photoionisation results [11] indicated that $^3CH_4(2)$ is much more populated than $^1CH_4(2)$ owing to the Franck–Condon factors. $^1CH_4(2)$ was dissociated into three fragments, i.e. $CH_2^+(^2A_1)$, $H^+(^1S)$ and $H(^2S)$, consistent with the present optimised geometries: at the CCSD(T)/6-311++G(d,p) level, two C—H distances in $^1CH_4(2)$ are large (1.440 Å) while the other two are short enough to form direct bonds (1.125 Å). However, the stable $^1CH_4(2)$ structure cannot be located. Fainelli et al. [13] observed that the lower binding energies of the di-cation $CH_4(2)$ will dissociate via two-body Coulomb explosion, which corresponds to the $^3CH_4(2)$ structure (see Section 3.4).

The equilibrium geometries of the five stable $^MCH_4(n)$ structures are displayed in Figure 1, where the C—H distances are given at both the MP2/6-311++G(d,p) and

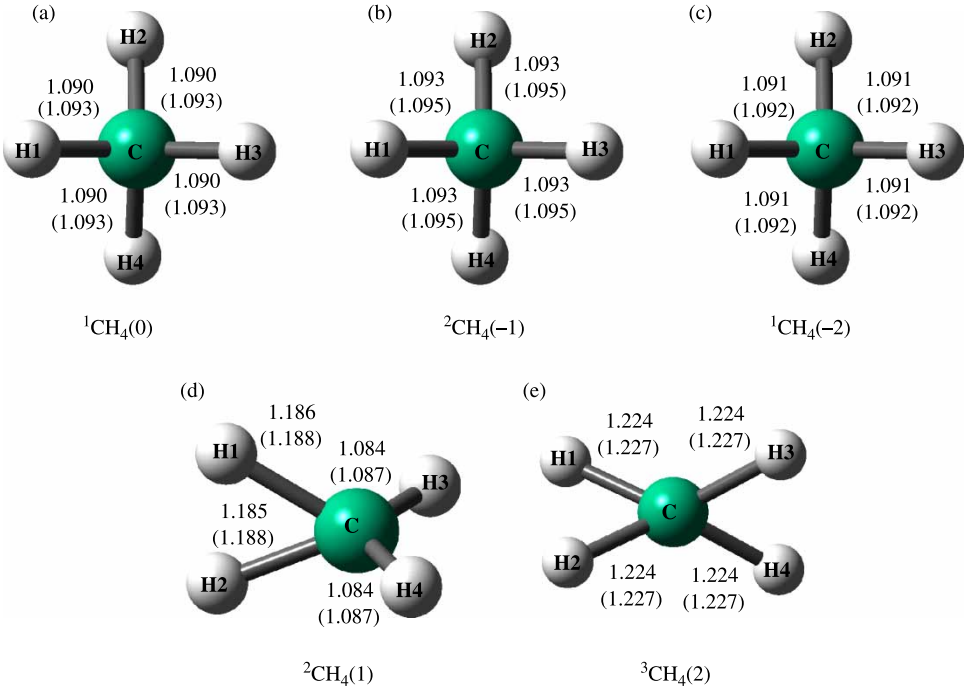

Figure 1. Presentations of the various $^MCH_4(n)$ structures. Distances were given at both the MP2/6-311++G(d,p) and CCSD(T)/6-311++G(d,p) (in parentheses) theoretical levels.

Table 1. The bond orders of the $^{M}CH_4(n)$ structures obtained at the CCSD(T)/6-311++G(d,p) theoretical level.

	$^1CH_4(0)$	$^2CH_4(-1)$	$^1CH_4(-2)$	$^2CH_4(1)$	$^3CH_4(2)$
C—H1	0.806	0.965	0.930	0.594	0.528
C—H2	0.806	0.965	0.930	0.594	0.528
C—H3	0.806	0.965	0.930	0.932	0.528
C—H4	0.806	0.965	0.930	0.932	0.528
H1—H2	0.004	0.052	0.156	0.128	0.037
H1—H3	0.004	0.052	0.156	0.001	0.001
H1—H4	0.004	0.052	0.156	0.001	0.001

CCSD(T)/6-311++G(d,p) levels. At the CCSD(T) level, the C—H bond lengths in $^1CH_4(0)$ were all equal to 1.093 Å. In the negatively charged $^2CH_4(-1)$ and $^1CH_4(-2)$ structures, the C—H distances were very close to those of $^1CH_4(0)$, with the largest deviations not more than 0.02 Å. In addition, the T_d molecular symmetry of $^1CH_4(0)$ was well preserved in $^2CH_4(-1)$ and $^1CH_4(-2)$. On the contrary, the positively charged $^2CH_4(1)$ and $^3CH_4(2)$ structures showed remarkable deviations from $^1CH_4(0)$. At the CCSD(T)/6-311++G(d,p) level, two C—H bonds in $^2CH_4(1)$ were elongated to 1.188 Å whereas the other two were slightly shortened; the four C—H bonds in $^3CH_4(2)$ were uniformly stretched to 1.227 Å. In $^2CH_4(1)$ and $^3CH_4(2)$, the H1–H2 distances were optimised at 1.102 and 1.438 Å, respectively, indicating strong interactions present in the two H atoms.

The C—H bond orders of the various $^{M}CH_4(n)$ structures are calculated and listed in Table 1. In comparison with the neutral $^1CH_4(0)$, the average C—H bond orders were increased in the anionic states but decreased in the ionic states. There were one or two net charges in $^2CH_4(-1)$ or $^1CH_4(-2)$, respectively; however, $^2CH_4(-1)$ instead of $^1CH_4(-2)$ was found to have the largest C—H bond orders. This may be due to the fact that more electron clouds in $^1CH_4(-2)$ are distributed along the H—H directions, as deduced from the H—H bond orders in Table 1. As the $^{M}CH_4(n)$ structures contain different charges, the bond-order analysis may fail to provide more information on the C—H interacting strengths, which will be discussed in Section 3.4 using BDE1s.

3.2 *Molecular orbital analysis*

Figure 2 illustrates the molecular orbital energies and symmetries of the five stable $^{M}CH_4(n)$ structures. $^1CH_4(0)$ has three energy levels, and the HOMOs are triply degenerate, both of which are in good agreement with the binding energy spectral and previous theoretical results [22,23]. The energy of its core orbital ($1a_1$) was calculated to be −304.95 eV (−11.21 a.u.) and was consistent with the value of −304.87 eV obtained by Wang [23] using the restricted Hartree–Fock method and the DGauss triple zeta with valence polarised basis set. The energies of the other orbitals also agree well with the previous data [22–24] and will not be elaborated. It was found from Figure 2 that the charges produce evident effects on both energies (E_{MO}) and symmetries. As the HOMOs of $^1CH_4(0)$ are threefold degenerate, its cations $^2CH_4(1)$ and $^3CH_4(2)$ are distorted by the strong Jahn–Teller effects and thus severely destabilised [7,8,10,11]. The hybrid orbitals formed with H_{1s} and $C_{2s,2p}$ are no longer degenerate. In $^3CH_4(2)$, two HOMOs are of close energies. All the occupied orbitals in $^3CH_4(2)$ are split into different energies. As for $^2CH_4(-1)$ and $^1CH_4(-2)$, their (HOMO−1)s are triply degenerate, resembling the HOMOs of $^1CH_4(0)$. The energies of all the orbitals are much altered due to the attachments of electrons. The HOMO of $^2CH_4(-1)$ is filled with one electron whose energy is positive (1.12 eV, i.e. 0.04 a.u.). The attachment of another electron into the HOMO of $^2CH_4(-1)$ forms $^1CH_4(-2)$ whose HOMO energy is greatly enhanced to 4.54 eV (0.17 a.u.). Accordingly, the attachment of electrons to the neutral $^1CH_4(0)$ becomes difficult, especially with doubly charged electrons [14].

3.3 *IEs and EAs*

The equilibrium adiabatic IEs and EAs of the neutral $^1CH_4(0)$ structure were derived from the expressions (2)–(5):

$$^1CH_4(0) \rightarrow {}^2CH_4(1) + e$$

$$IE1 = E[^2CH_4(1)] - E[^1CH_4(0)], \quad (2)$$

$$^2CH_4(1) \rightarrow {}^3CH_4(2) + e$$

$$IE2 = E[^3CH_4(2)] - E[^2CH_4(1)], \quad (3)$$

$$^2CH_4(-1) \rightarrow {}^1CH_4(0) + e$$

$$EA1 = E[^1CH_4(0)] - E[^2CH_4(-1)], \quad (4)$$

$$^1CH_4(-2) \rightarrow {}^2CH_4(-1) + e$$

$$EA2 = E[^2CH_4(-1)] - E[^1CH_4(-2)]. \quad (5)$$

The energies of the $^{M}CH_4(n)$ structures were obtained at their respective equilibrium geometries. IE1 and IE2 are the first and second IEs of the neutral $^1CH_4(0)$ structure. EA1 and EA2 are its first and second EAs, respectively.

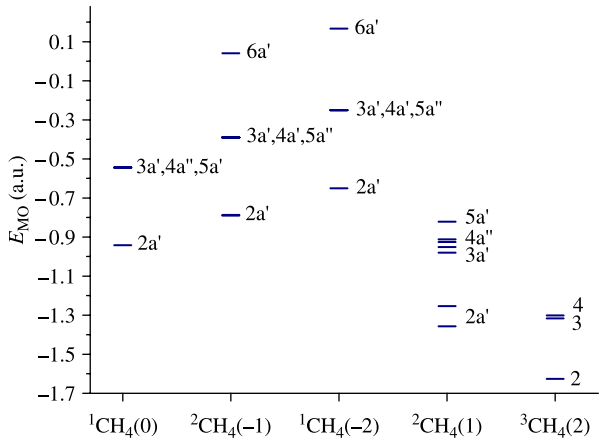

Figure 2. Molecular orbital energies of the various $^{M}CH_4(n)$ structures calculated at the MP2/6-311++G(d,p) level of theory. The energies of C_{1s} orbitals remain nearly invariant in all the cases and are not shown.

The calculated IE1, IE2, EA1 and EA2 of $^1CH_4(0)$ are listed in Table 2. For comparison, the corresponding data of the isoelectronic Ne were also obtained at the same level, and it was found that the ionisations and attachments of electrons were always more facile for $^1CH_4(0)$ rather than Ne. The first IE1 of $^1CH_4(0)$ was calculated to be 12.57 eV. Chupka and Berkowitz [9] measured the relative photoionisation cross-section of $^1CH_4(0)$ at liquid N_2 temperature and concluded that its IE1 value should not exceed 12.615 ± 0.01 eV. Boyd et al. [7] extrapolated the IE1 value of 12.51 eV on the basis of high-resolution He I photoelectron spectrum. These results are consistent with the present data. The first EA1 of $^1CH_4(0)$ is equal to −0.98 eV and indicates that the attachment of one electron is endothermic. The attachment of the second electron to $^1CH_4(0)$ seems extremely difficult, costing an energy of 4.00 eV. The corresponding EA1 and EA2 values of Ne are much larger than those of $^1CH_4(0)$. The IE1 and IE2 values of Ne are also very large. The calculated IE1 value of Ne (21.16 eV) is in good agreement with the recommended value 21.564 eV [25]. Albeit that the noble gas Ne was considered very inert, the advances of experimental techniques have witnessed the successful syntheses of many noble-gas contained compounds [26–29].

3.4 *The first C—H BDE1s of the $^{M}CH_4(n)$ structures*

For each of the $^1CH_4(0)$, $^2CH_4(-1)$, $^1CH_4(-2)$, $^2CH_4(1)$ and $^3CH_4(2)$ structures, several dissociation pathways of the first C—H bonds may exist with the $^{M1}CH_3(n1)$ and $^{M2}H(n2)$ products of different charges and spin multiplicities. Using Equation (1), the first C—H BDE1s of all the possible pathways were calculated, with those of the lowest BDE1 values shown below:

$$^1CH_4(0) \rightarrow {}^2CH_3(0) + {}^2H(0), \quad (6)$$

$$^2CH_4(-1) \rightarrow {}^2CH_3(0) + {}^1H(-1), \quad (7)$$

$$^1CH_4(-2) \rightarrow {}^1CH_3(-1) + {}^1H(-1), \quad (8)$$

$$^2CH_4(1) \rightarrow {}^1CH_3(1) + {}^2H(0), \quad (9)$$

$$^3CH_4(2) \rightarrow {}^1CH_3(1) + {}^1H(1). \quad (10)$$

The dissociation pathways of $^2CH_4(1)$ and $^3CH_4(2)$ in Equations (9) and (10) were supported by the previous experimental results: CD_3^+ is the most abundant fragment by dissociating $^2CD_4(1)$ [30]. The dissociation of $^3CH_4(2)$ into $^1CH_3(1) + {}^1H(1)$ was confirmed as the most favourable pathway [11]. There is also evidence for the negatively charged $^2CH_4(-1)$ and $^1CH_4(-2)$: $^1H(-1)$ other than $^2H(0)$ or $^1H(1)$ was detected in the dissociation processes of electron-attached methane structures [14].

The BDE1 values corresponding to Equations (6)–(10) are calculated and listed in Table 3. The BDE1 of $^1CH_4(0)$ equals 106.22 kcal mol^{-1} at the MP2/6-311++G(d,p) or 107.68 kcal mol^{-1} at the CCSD(T)/6-311++G(d,p) levels, in agreement with the experimental value 105.0 ± 0.1 kcal mol^{-1} [31]. The BDE1s of the five $^{M}CH_4(n)$ structures increase in the order $^3CH_4(2) < {}^1CH_4(-2) < {}^2CH_4(1) < {}^2CH_4(-1) < {}^1CH_4(0)$. It was found that the first C—H bonds are much activated when the neutral $^1CH_4(0)$ is endowed with charges. The C—H bond dissociations are even exothermic in $^1CH_4(-2)$ and $^3CH_4(2)$, quite contrary to the conventional activation methods where a great deal of energies were used to break the first C—H bonds [15–18].

Table 2. IEs and EAs of CH_4 and Ne obtained at the CCSD(T)/6-311++G(d,p) level of theory.[a]

	IE1	IE2	EA1	EA2
CH_4	12.57	20.21	−0.98	−4.00
Ne	21.16	44.10	−7.35	−14.44

[a] Units of energies in eV.

3.5 *$^1CH_4(0)$ bound to anions and cations: a comparison*

The complexes of $^1CH_4(0)$ bound to anions (O^{2-} and F^-) and cations (Na^+ and Mg^{2+}) were studied by the MP2/6-311++G(d,p) methods. Ferrari et al. [32] compared the different binding modes between $^1CH_4(0)$ and cations (Na^+ and Mg^{2+}), concluding that the threefold one is the most energetically favourable. Accordingly, the threefold binding mode with cations was considered in this work; see the optimised geometries in Figure 3(c) and (d). In the threefold binding mode, three H atoms (H1–H3) have identical distances towards the cations and the fourth H atoms (H4) are directed opposite: in $^1CH_4(0)$—Na^+ and $^1CH_4(0)$—Mg^{2+}, the ∠H4—C—Na and ∠H4—C—Mg angles were optimised at 179.83° and 179.90°, respectively. The C—H1, H2, H3 and C—H4 distances are equal

Table 3. The first C—H BDE1s of the various structures.[a]

	$^1CH_4(0)$	$^2CH_4(-1)$	$^1CH_4(-2)$	$^2CH_4(1)$	$^3CH_4(2)$	$^2CH_3(0)$
MP2	106.22	79.71	−5.15	38.10	−163.34	110.66
CCSD(T)	107.68	75.56	−3.77	38.24	−164.16	110.94
Exp.[b]	105.0 ± 0.1					110.3

[a] Units of energies in kcal mol^{-1}.
[b] Experimental data from [31].

to 1.095 (1.094) and 1.089 (1.088) Å in $^1CH_4(0)$—Na^+ and 1.109 (1.108) and 1.103 (1.106) Å in $^1CH_4(0)$—Mg^{2+}, respectively. The values in parentheses were obtained by Ferrari et al. [32] at the B3LYP/TZV level of theory, which are found to be in agreement with the present results. In comparison with the neutral $^1CH_4(0)$ (Figure 1(a)), the C—H bond distances change slightly in $^1CH_4(0)$—Na^+ whereas they are elongated by ca. 0.014(5) Å in $^1CH_4(0)$—Mg^{2+}. The C—Na and C—Mg distances equal 2.638 and 2.168 Å, respectively, close to the values of 2.519 and 2.162 Å obtained by Ferrari et al. [32]. The direct C—Mg bonds were formed and therefore the MP2 and B3LYP data are almost identical; however, the C—Na distance is larger than that expected for the direct bonds and the mutual interactions may be improperly described by density functional methods [33–35], due to their inadequacies of exchange functional.

The interaction modes between $^1CH_4(0)$ and anions (O^{2-} and F^-) were explored and the stable structures are shown in Figure 3(a) and (b). It was found that the H1 atoms were directed towards the anions with the ∠H1—C—O and ∠H1—C—F angles equal to 179.88° and 179.98°, respectively. Owing to the polarisations by the anions, the C—H1 bonds are more stretched than the other three. Compared with the neutral $^1CH_4(0)$ (Figure 1(a)), all the C—H bonds in $^1CH_4(0)$—O^{2-} are much elongated, whereas only the C—H1 bond has observable elongations in $^1CH_4(0)$—F^-. The O—H1 and F—H1 distances were calculated at 1.525 and 1.924 Å, respectively.

The BDE1 values of the structures of $^1CH_4(0)$ bound to anions (O^{2-} and F^-) and cations (Na^+ and Mg^{2+}) were obtained in the same way as the $^MCH_4(n)$ structures described above. The most favourable dissociation pathways were thus determined:

$$^1CH_4(0)—O^{2-} \rightarrow {}^1CH_3(-1) + OH^-, \quad (11)$$

$$^1CH_4(0) - F^- \rightarrow {}^1CH_3(-1) + HF, \quad (12)$$

$$^1CH_4(0) - Na^+ \rightarrow {}^2CH_3(0) + {}^2H(0) + Na^+, \quad (13)$$

$$^1CH_4(0) - Mg^{2+} \rightarrow {}^1CH_3(-1) - Mg^{2+} + {}^1H(1). \quad (14)$$

The first C—H BDE1s were computed at −72.18, 59.94, 104.54 and 82.15 kcal mol^{-1} for $^1CH_4(0)$—O^{2-}, $^1CH_4(0) - F^-$, $^1CH_4(0)$—Na^+ and $^1CH_4(0)$—Mg^{2+}, respectively. It was found that the interactions with O^{2-}, F^- or Mg^{2+} dramatically reduced the BDE1 values, thus

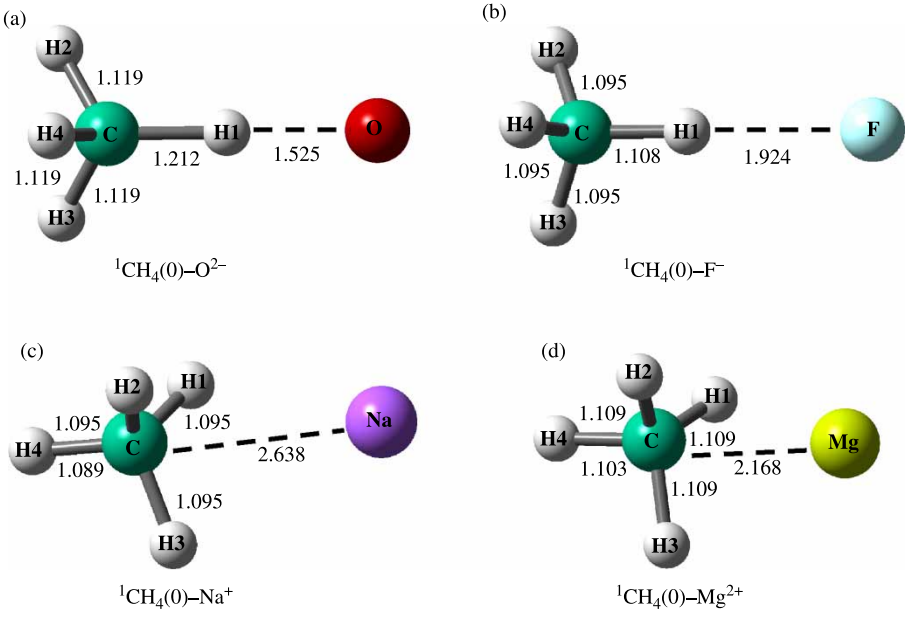

Figure 3. Structures of $^1CH_4(0)$ bound to anions and cations. The distances were given at the MP2/6-311++G(d,p) level of theory.

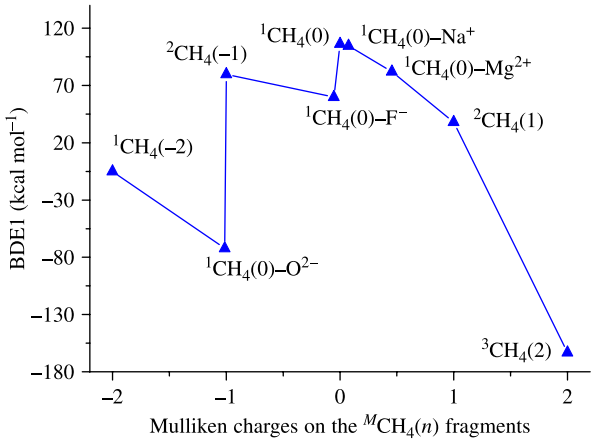

Figure 4. The first C—H BDE1 of methane under different chemical environments obtained at the MP2/6-311++G(d,p) level of theory.

activating the methane molecules. The affinities of O^{2-} towards $^1CH_4(0)$ were found to be different from those of $O(^1D)$ and $O(^3P)$. The insertion of $O(^1D)$ into the C—H bonds of $^1CH_4(0)$ is barrierless [36–38], and the H1—O distance in the $O(^3P)$-bound $^1CH_4(0)$ structure was optimised to be 2.991 Å [39], much longer than the corresponding value in $^1CH_4(0)$—O^{2-}.

The Mulliken charges of the $^1CH_4(0)$ fragments were calculated at −1.013, −0.054, 0.076 and 0.456 $|e|$ in $^1CH_4(0)$—O^{2-}, $^1CH_4(0)$—F^-, $^1CH_4(0)$—Na^+ and $^1CH_4(0)$—Mg^{2+}, respectively. It was found that the charges were affected by the affinities of anions and cations. Figure 4 charted the first C—H BDE1s of the various structures versus the charges of the $^1CH_4(0)$ fragments. Generally, the more the deviations of the charges from zero, i.e. the charge in the neutral $^1CH_4(0)$ structure, the larger the activations of the first C—H bonds. Na^+ reduced the charge very slightly (0.076 $|e|$) and therefore only a slight energy drop (1.68 kcal mol^{-1}) was observed. $^1CH_4(0)$—O^{2-} is an exception and the reason may be that the dissociated product OH^- is exceptionally stable. Therefore, the charge effects can be used to direct the activations of C—H bonds in alkanes.

3.6 The selective activations of methane by charge effects

The BDE2s, i.e. the C—H BDE1s of the $^{M1}CH_3(n1)$ structures, were obtained in the same way as the $^MCH_4(n)$ structures. Now we know the first and second C—H dissociation steps of the $^MCH_4(n)$ structures: $^1CH_4(0) \rightarrow {}^2CH_3(0) \rightarrow {}^3CH_2(0)$, $^2CH_4(-1) \rightarrow {}^2CH_3(0) \rightarrow {}^3CH_2(0)$, $^1CH_4(-2) \rightarrow {}^1CH_3(-1) \rightarrow {}^3CH_2(0)$, $^2CH_4(1) \rightarrow {}^1CH_3(1) \rightarrow {}^2CH_2(1)$ and $^3CH_4(2) \rightarrow {}^1CH_3(1) \rightarrow {}^2CH_2(1)$.

$^2CH_2(-1)$ may also appear in the dissociated products of the second step of $^1CH_4(-2)$, since the BDE2 value dissociated in this way is only 6.67 kcal mol^{-1} beyond the most favourable pathway producing $^3CH_2(0)$. In the favourable dissociation pathway $[^1CH_4(-2) \rightarrow {}^1CH_3(-1) \rightarrow {}^3CH_2(0)]$, $^2H(-1)$ is the product of both steps. It is thus consistent with the dissociative electron attachment results [14] that the $^2H(-1)$ channel corresponds to a fairly broad peak whereas $^2CH_2(-1)$ to a relatively narrow peak.

The C—H BDE1s of the $^2CH_3(0)$ structures were calculated at 110.66 and 110.94 kcal mol^{-1} at the MP2/6-311++G(d,p) and CCSD(T)/6-311++G(d,p) levels, respectively, in accord with the experimental value 110.3 kcal mol^{-1} [31].

As for the $^MCH_4(n)$ structures, the differences between the BDE1s and BDE2s were defined as follows:

$$\Delta BDE = BDE2 - BDE1. \quad (15)$$

As shown in Figure 5, the ΔBDE values obtained at the CCSD(T)/6-311++G(d,p) level increase in the order of 3.26 kcal mol^{-1} for $^1CH_4(0) <$ 35.38 kcal mol^{-1} for $^2CH_4(-1) <$ 87.09 kcal mol^{-1} for $^2CH_4(1) <$ 92.42 kcal mol^{-1} for $^1CH_4(-2) <$ 289.49 kcal mol^{-1} for $^3CH_4(2)$. The ΔBDE value in the neutral $^1CH_4(0)$ structure is so slight that the H-abstraction reactions are not easily controlled at the level of the first C—H bonds. By attaching or ionising the electrons, the ΔBDE values become remarkably larger, indicating that the selective activations of methane have been achieved. The first and second C—H bond activation reactions in $^1CH_4(-2)$ and $^3CH_4(2)$ are even exothermic and endothermic, respectively.

At the CCSD(T)/6-311++G(d,p) level, the computational C—H and O—H BDE1s of methanol (CH_3OH) are equal to 99.82 and 106.96 kcal mol^{-1}, consistent with the experimental results of 96.06 ± 0.15 and 104.2 ±

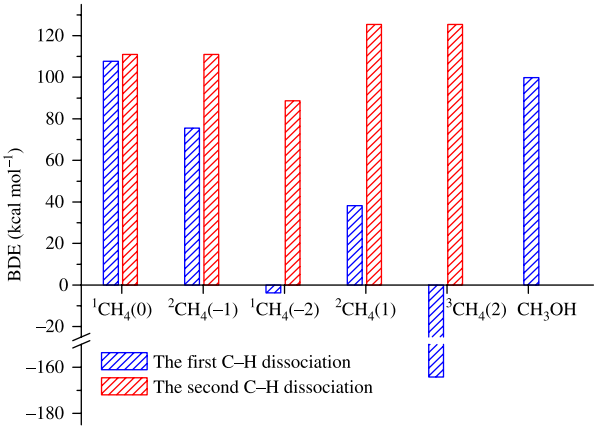

Figure 5. The first C—H BDE1 of the various $^MCH_4(n)$ structures and CH_3OH obtained at the CCSD(T)/6-311++G(d,p) theoretical level.

$0.9\,\mathrm{kcal\,mol^{-1}}$ [31], respectively. As expected, the C—H bond BDE1 of methanol is less than the BDE1 of the neutral $^1CH_4(0)$. However, the situation will be changed by charge effects. Since the activations of the first C—H bonds in $^1CH_4(-2)$, $^2CH_4(1)$ and $^3CH_4(2)$ require much less energies than those of methanol (CH_3OH), it is facile to control the reaction directions by selective activations of the first C—H bonds in methane rather than the deeper oxidisations of methanol (CH_3OH).

The differences of the BDE1s between the second C—H bonds of the $^MCH_4(n)$ structures and the first C—H bond of methanol were defined as follows:

$$\Omega\mathrm{BDE} = \mathrm{BDE2} - \mathrm{BDE}(CH_3OH). \qquad (16)$$

The ΩBDE values increase in the order of $-11.17\,\mathrm{kcal\,mol^{-1}}$ for $^1CH_4(-2) < 11.12\,\mathrm{kcal\,mol^{-1}}$ for $^2CH_4(-1) < 25.51\,\mathrm{kcal\,mol^{-1}}$ for $^2CH_4(1) = 25.51\,\mathrm{kcal\,mol^{-1}}$ for $^3CH_4(2)$. The activation of the second C—H bond in $^1CH_4(-2)$ was found to be preferred over the C—H bond in methanol (CH_3OH); while in $^2CH_4(-1)$, $^2CH_4(1)$ and $^3CH_4(2)$, the C—H bond activation in methanol (CH_3OH) is preferred. Accordingly, through the attachment or ionisation of different electrons, the reaction directions posterior to the first C—H bond activation can also be fine-tuned.

There are currently two known primary problems restricting the methane conversions: one is the difficult activation of the first C—H bonds, and the other is the easier activation of those products more desirable than methane such as methanol. These two problems can be resolved with charge effects. As for the first problem, the charge effects greatly reduce the activation energies of methane. As for the second problem, the appropriate charge effects can decide the reaction directions towards the C—H activation of methane or the activation of the product methanol (CH_3OH). In addition, through the charge effects, the reactions can be well controlled at the levels of the first C—H bond activations instead of the further C—H bond activations, since in the charged structures, the energies required to break the first C—H bonds are much less than and also far away from the values to break the second C—H bonds. After the first C—H bond activations in methane, two alternatives remain: the activation of the second C—H bonds or the further activation of the product methanol (CH_3OH). The charge effects can switch the alternatives: the activation of the second C—H bond in $^1CH_4(-2)$ is preferred over that in methanol (CH_3OH), while in $^2CH_4(-1)$, $^2CH_4(1)$ and $^3CH_4(2)$, the C—H bond activation in methanol (CH_3OH) is preferred. The present results of selective activations of methane with charge effects are of high value to the effective utilisations of alkanes.

4. Conclusions

The neutral methane structures endowed with both positive and negative charges have been observed experimentally; however, the understanding of these charged structures is rather limited. With the aid of *ab initio* calculations, systematic work was carried out on the $^MCH_4(n)$ structures as well as on the structures of $^1CH_4(0)$ bound to anions and cations.

The stable $^MCH_4(n)$ structures ($n = 0, \pm 1, \pm 2$) were determined, corresponding to $^1CH_4(0)$, $^2CH_4(-1)$, $^1CH_4(-2)$, $^2CH_4(1)$ and $^3CH_4(2)$, respectively. The geometries and the T_d molecular symmetries of the neutral $^1CH_4(0)$ are well reserved in the negatively charged structures but severely distorted in the positively charged. Owing to the strong Jahn–Teller effects, the cations and anions of $^1CH_4(0)$ are unstable, and their molecular orbital energies and symmetries are also altered compared with those of $^1CH_4(0)$. The HOMO energies of $^2CH_4(-1)$ and $^1CH_4(-2)$ are beyond zero, an indication of the structural instabilities. The first and second IEs and EAs were calculated for $^1CH_4(0)$ and the isoelectronic Ne, which are in good agreement with the available data.

The binding modes of $^1CH_4(0)$ with cations (Na^+ and Mg^{2+}) and anions (O^{2-} and F^-) are threefold and onefold, respectively. Strong interactions are present between the O^{2-} and H1 atoms in $^1CH_4(0)$—O^{2-} as well as the Mg^{2+} and C atoms in $^1CH_4(0)$—Mg^{2+}. As for the C—H bonds, the most marked elongations were observed in $^1CH_4(0)$—O^{2-} whereas on the contrary in $^1CH_4(0)$—Na^+.

According to the C—H BDE1s, the dissociation pathways of the $^MCH_4(n)$ structures are as follows: $^1CH_4(0) \rightarrow {}^2CH_3(0) \rightarrow {}^3CH_2(0)$, $^2CH_4(-1) \rightarrow {}^2CH_3(0) \rightarrow {}^3CH_2(0)$, $^1CH_4(-2) \rightarrow {}^1CH_3(-1) \rightarrow {}^3CH_2(0)$, $^2CH_4(1) \rightarrow {}^1CH_3(1) \rightarrow {}^2CH_2(1)$ and $^3CH_4(2) \rightarrow {}^1CH_3(1) \rightarrow {}^2CH_2(1)$, which are in good agreement with the available experimental data. The C—H bond dissociation mechanisms of the structures of $^1CH_4(0)$ bound to anions and cations were studied as well; see the details in Section 3. It was thus revealed that the first C—H BDE1s of the various structures are to a large extent determined by the charges of the $^1CH_4(0)$ fragments: the more deviations from zero tend to cause more reductions in the BDE1s values.

The difficult activation of the first C—H bonds and the easier activation of those products more desirable than methane are the two primary problems that restrict the current methane utilisations; these can be satisfactorily resolved with charge effects. In addition, through the charge effects, the reactions can be well controlled at the level of the first C—H bond breaking instead of the further C—H bond breaking. Moreover, the alternatives as to activating the second C—H bonds of methane or the product methanol (CH_3OH) can also be switched through the charge effects.

Acknowledgements

This work was financially supported by the Ministry of Science and Technology of China (No. 2005CB221405), Major State Basic Research Development Programs (No. 2004CB719902) and National Natural Science Foundation (No. 20633060).

References

[1] K.D. Jordan, *Negative ion states of polar molecules*, Acc. Chem. Res. 12 (1979), pp. 36–42.
[2] G.L. Gutsev and L. Adamowicz, *Electronic and geometrical structure of dipole-bound anions formed by polar molecules*, J. Phys. Chem. 99 (1995), pp. 13412–13421.
[3] D.M.A. Smith, J. Smets, Y. Elkadi, and L. Adamowicz, Ab initio *theoretical study of dipole-bound anions of molecular complexes. Water trimer anion*, J. Chem. Phys. 107 (1997), pp. 5788–5793.
[4] M. Gutowski, P. Skurski, and J. Simons, *Dipole-bound anions of glycine based on the zwitterion and neutral structures*, J. Am. Chem. Soc. 122 (2000), pp. 10159–10162.
[5] L.R. Santiago, M. Sodupe, A. Oliva, and J. Bertran, *Intramolecular proton transfer in glycine radical cation*, J. Phys. Chem. A 104 (2000), pp. 1256–1261.
[6] H.Q. Ai, Y.X. Bu, P. Li, and Z.Q. Li, *Fragmentation and deformation mechanism of glycine isomers in gas phase: Investigations of charge effect*, J. Chem. Phys. 120 (2004), pp. 11600–11614.
[7] R.J. Boyd, K.V. Darvesh, P.D. Fricker, *Energy component analysis of the Jahn–Teller effect in the methane radical cation*, J. Chem. Phys. 94 (1991), pp. 8083–8088.
[8] I.B. Bersuker, *Modern aspects of the Jahn–Teller effect theory and applications to molecular problems*, Chem. Rev. 101 (2001), pp. 1067–1114.
[9] W.A. Chupka and J. Berkowitz, *Photoionization of methane: Ionization potential and proton affinity of CH_4*, J. Chem. Phys. 54 (1971), pp. 4256–4266.
[10] J.W. Rabalais, T. Bergmark, L.O. Werme, L. Karlsson, and K. Siegbahn, *The Jahn–Teller effect in the electron spectrum of methane*, Phys. Scr. 3 (1971), pp. 13–18.
[11] G. Dujardin, D. Winkoun, and S. Leach, *Double photoionization of methane*, Phys. Rev. A 31 (1985), pp. 3027–3038.
[12] D. Stahl, F. Maquin, T. Gäumann, H. Schwarz, P.A. Carrupt, and P. Vogel, *Experimental and* ab initio *molecular orbital studies on collisions of methane radical ion(1^+) (CH_4^+.cntdot.) and monoprotonated methane (CH_5^+) with molecular oxygen: On the formation of methane (CH_4^{2+}) and methonium (CH_5^{2+}) dications and stable CHn-species (n = 0–3)*, J. Am. Chem. Soc. 107 (1985), pp. 5049–5053.
[13] E. Fainelli, G. Alberti, R. Flammini, F. Maracci, P. Bolognesi, M. Mastropietro, and L. Avaldi, *Fragmentation of CH_4^{2+} following C 1s ionisation studied by Auger electron–ion–ion coincidence experiments*, J. Electron Spectrosc. Relat. Phenom. 161 (2007), pp. 51–57.
[14] P. Rawat, V.S. Prabhudesai, M.A. Rahman, N.B. Ram, and E. Krishnakumar, *Absolute cross sections for dissociative electron attachment to NH_3 and CH_4*, Int. J. Mass Spectrom. 227 (2008), pp. 96–102.
[15] T.V. Choudhary, E. Aksoylu, and D.W. Goodman, *Non-oxidative activation of methane*, Catal. Rev. 45 (2003), pp. 151–203, and references therein.
[16] A.T. Ashcroft, A.K. Cheetham, J.S. Foord, M.L.H. Green, C.P. Grey, A.J. Murrell, and P.D.F. Vernon, *Selective oxidation of methane to synthesis gas using transition metal catalysts*, Nature 344 (1990), pp. 319–321.
[17] R.A. Periana, D.J. Taube, S. Gamble, H. Taube, T. Satoh, and H. Fujii, *Platinum catalysts for the high-yield oxidation of methane to a methanol derivative*, Science 280 (1998), pp. 560–564.
[18] S. Feyel, J. Döbler, D. Schröder, J. Sauer, and H. Schwarz, *Thermal activation of methane by tetranuclear $[V_4O_{10}]^+$*, Angew. Chem., Int. Ed. 45 (2006), pp. 4681–4685.
[19] M.J. Frisch, G.W. Trucks, H.B. Schlegel, G.E. Scuseria, M.A. Robb, J.R. Cheeseman, J.A. Montgomery T. Vreven Jr, K.N. Kudin, J.C. Burant, J.M. Millam, S.S. Iyengar, J. Tomasi, V. Barone, B. Mennucci, M. Cossi, G. Scalmani, N. Rega, G.A. Petersson, H. Nakatsuji, M. Hada, M. Ehara, K. Toyota, R. Fukuda, J. Hasegawa, M. Ishida, T. Nakajima, Y. Honda, O. Kitao, H. Nakai, M. Klene, X. Li, J.E. Knox, H.P. Hratchian, J.B. Cross, C. Adamo, J. Jaramillo, R. Gomperts, R.E. Stratmann, O. Yazyev, A.J. Austin, R. Cammi, C. Pomelli, J.W. Ochterski, P.Y. Ayala, K. Morokuma, G.A. Voth, P. Salvador, J.J. Dannenberg, V.G. Zakrzewski, S. Dapprich, A.D. Daniels, M.C. Strain, O. Farkas, D.K. Malick, A.D. Rabuck, K. Raghavachari, J.B. Foresman, J.V. Ortiz, Q. Cui, A.G. Baboul, S. Clifford, J. Cioslowski, B.B. Stefanov, G. Liu, A. Liashenko, P. Piskorz, I. Komaromi, R.L. Martin, D.J. Fox, T. Keith, M.A. Al-Laham, C.Y. Peng, A. Nanayakkara, M.P. Challacombe, M.W. Gill, B. Johnson, W. Chen, M.W. Wong, C. Gonzalez, and J.A. Pople, *Gaussian 03.1. Revision C.02*, Gaussian Inc, Wallingford, CT, 2004.
[20] E.D. Glendening, A.E. Reed, J.E. Carpenter, and F. Weinhold, *NBO Version 3.1*.
[21] K.B. Wiberg, *Application of the Pople–Santry–Segal CNDO method to the cyclopropylcarbinyl and cyclobutyl cation and to bicyclobutane*, Tetrahedron 24 (1968), pp. 1083–1096.
[22] S.A.C. Clark, T.J. Reddish, C.E. Brion, E.R. Davidson, and R.F. Frey, *The valence orbital momentum distributions and binding energy spectra of methane by electron momentum spectroscopy: Quantitative comparisons using near Hartree–Fock limit and correlated wavefunctions*, Chem. Phys. 143 (1990), pp. 1–10.
[23] F. Wang, *Molecular orbitals of methane: Symmetry or hybridization*, J. Mol. Struct. Theochem. 678 (2004), pp. 105–111.
[24] M.S. Banna, E.E. Mills, D.W. Davis, and D.A. Shirley, *X-ray photoemission molecular orbitals of hydrogen fluoride and the fluorinated methanes*, J. Chem. Phys. 61 (1974), pp. 4780–4786.
[25] http://web.mit.edu/course/3/3.091/www3/pt/pert9.html.
[26] H.H. Claassen, H. Selig, and J.G. Malm, *Production and reactions of methylene in the triplet state*, J. Am. Chem. Soc. 84 (1962), pp. 3593–3594.
[27] R. Hiller, K. Weninger, S.J. Putterman, and B.P. Barber, *Effect of noble gas doping in single-bubble sonoluminescence*, Science 248 (1994), pp. 248–250.
[28] L. Khriachtchev, M. Pettersson, N. Runeberg, J. Lundell, and M. Räsänen, *A stable argon compound*, Nature 406 (2000), pp. 874–877.
[29] S. Yockel, J.J. Seals, and A.K. Wilson, *An* ab initio *study of the noble gas compound HKrCl*, Chem. Phys. Lett. 393 (2004), pp. 448–452.
[30] A. Quyyum, W. Schustereder, C. Mair, T. Tepnual, P. Scheier, and T.D. Märk, *Ion surface collisions of CH_3^+, CH_4^+, CH_5^+ and CD_4^+*, Rad. Phys. Chem. 68 (2003), pp. 257–261.
[31] Y.R. Luo, *Handbook of Bond Dissociation Energies in Organic Compounds*, CRC Press, Boca Raton, FL, 2003.
[32] A.M. Ferrari, K.M. Neyman, S. Huber, H. Knözinger, and N. Rösch, *Density functional study of methane interaction with alkali and alkaline-earth metal cations in zeolites*, Langmuir 14 (1998), p. 5559–5567.
[33] M. Kamiya, T. Tsuneda, and K. Hirao, *A density functional study of van der Waals interactions*, J. Chem. Phys. 117 (2002), pp. 6010–6015.
[34] B. Santra, A. Michaelides, and M. Scheffler, *On the accuracy of density-functional theory exchange-correlation functionals for H bonds in small water clusters: Benchmarks approaching the complete basis set limit*, J. Chem. Phys. 127 (2007), 184104.
[35] G. Yang, Y.G. Zu, C.B. Liu, Y.J. Fu, and L.J. Zhou, *Stabilization of amino acid zwitterions with varieties of anionic species: The intrinsic mechanism*, J. Phys. Chem. B 112 (2008), pp. 7104–7110.
[36] A.H.H. Chang and S.H. Lin, *A theoretical study of the $O(^1D) + CH_4$ reaction I*, Chem. Phys. Lett. 363 (2002), pp. 175–181.
[37] H. Jordi, M. Judith, R. Sayós, and M. González, Ab initio *study of the $O(^1D) + CH_4(X^1A_1) \rightarrow OH(X^2\prod) + CH_3(X^2A^{112})$ reaction: Ground and excited potential energy surfaces*, J. Chem. Phys. 119 (2003), pp. 9504–9512.
[38] H.G. Yu and J.T. Mucherman, *MRCI calculations of the lowest potential energy surface for CH_3OH and direct* ab initio *dynamics simulations of the $O(^1D) + CH_4$ reaction*, J. Phys. Chem. A 108 (2004), pp. 8615–8623.
[39] D. Troya, R.Z. Pascual, and G.C. Schztz, *Theoretical Studies of the $O(^3P) +$ methane reaction*, J. Phys. Chem. A 107 (2003), pp. 10497–10506.